Arab J Geosci (2009) 2:1–17
DOI 10.1007/s12517-008-0008-y

ORIGINAL PAPER

Mineralogy and mineral chemistry of auriferous stream sediments from Al Wajh area, NW Saudi Arabia

A. M. B. Moufti

Received: 28 July 2008 / Accepted: 28 July 2008 / Published online: 23 December 2008

Abstract A detailed ore microscopic study strengthened by fire assay data of Al Wajh stream sediments (Wadi Al Miyah, Wadi Haramil and Wadi Thalbah) in northwestern Saudi Arabia shows economic concentrations of gold in the silt fraction (40–63 μm). However, particles of extremely fine "dusty" gold (≤40 μm in size) were also identified in most stations as independent grains. The maximum gold content in the samples of Wadi Al Miyah is 13.61 wt%, which is reported for the heavy fraction (<40 μm). Maximum gold content in the heavy fractions of Wadi Haramil stream sediments amounts 6.90 g/t Au in a relatively coarse fraction (63–125 μm). It appears that the most fertile heavy fraction in gold among the analysed samples are those from Wadi Thalbah that have the highest index figure, which makes the placer gold in them more profitable from the economic point of view. The gold content in the heavy fractions of samples from Wadi Thalbah is economically high lying in the range 6.27–28.83 g/t Au, except for a sample collected at the upstream with 0.77 g/t Au. Al Wajh stream sediments (including the beach light and black sands) are also rich in Fe–Ti oxides, rutile and zircon, whereas monazite and thorite are much lesser. Mineral chemistry of magnetite indicates a distinct titanomagnetite variety (with 3.85 wt% TiO_2) which is consistent with the ore microscopic investigation. The titanomagnetite is V- and Cr-free, which indicates derivation from a more felsic source than a mafic one. No traces of U were found in zircon that sometimes bears up to 2.74 wt% Hf_2O_3. Chemical analyses of monazite show typical common contents of rare earth elements such as La, Ce, Nd and Sm. Thorite is either U-free or uranothorite varieties where the latter contains up to 31.79 wt% UO_2. One of the U-free thorite grains is Y-bearing and contains 7.13 wt% Y_2O_3.

Keywords Al Wajh area · Auriferous stream sediments · NW Saudi Arabia

A. M. B. Moufti (✉)
Department of Mineral Resources and Rocks,
Faculty of Earth Sciences, King Abdulaziz University,
B.O.Box 80206, Jeddah 21589, Saudi Arabia
e-mail: ambmoufti@hotmail.com

Introduction

The present paper sheds light on the mineralogical and geochemical characteristics of stream sediments in three wadis in northwestern (NW) Saudi Arabia. In this context, the authors give an extensive trial to have a reasonable coverage of sampling in order to have collective idea about sediments in the three surveyed wadis from the upstream to the downstream. Aiming to have detailed information about the mineralogical composition of the fractions of auriferous sediments (i.e. that bear gold), the samples were subjected to heavy mineral separation that was followed by detailed microscopic study and finally the determination of their gold contents.

The studied stream sediments are located between Al Wajh and Duba in NW Kingdom of Saudi Arabia (Fig. 1) at Wadi Al Miyah, Wadi Haramil and Wadi Thalbah. Systematically, the work started with careful selection of samples with the documentation of their exact locations using a modern global positioning system, followed by plotting on recent satellite images (Google Images 2008).

During the last two decades, gold exploration in the stream sediments attracted several workers including those of the US Geological Survey missionary campaigns, in addition to houses of expertise and consultations. Qadi et

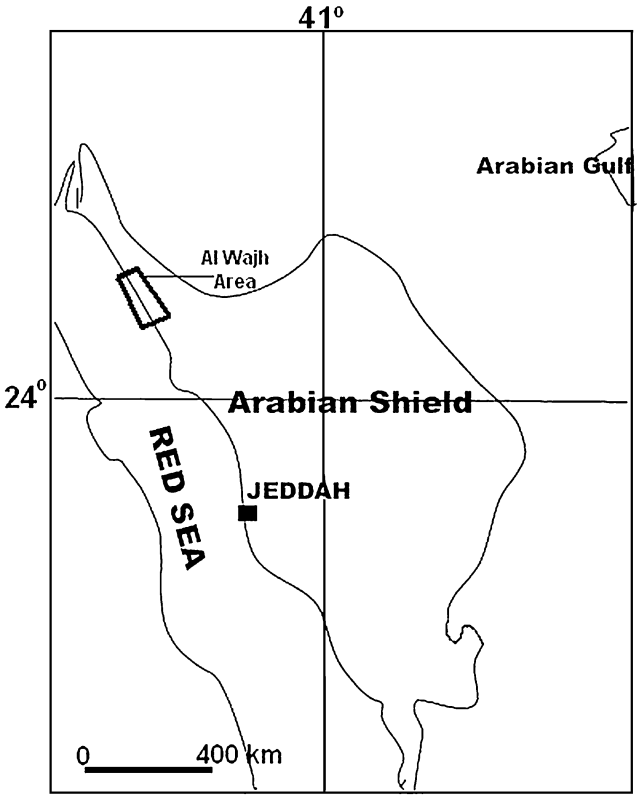

Fig. 1 Location map of the study area

al. (2007) presented a review for placer gold exploration in the stream sediments of Saudi Arabia and mentioned that limited ancient activities for placer gold extraction was known in the vicinity of low-grade quartz veins at Hamdah, Ad Duwayhi, Mahd Ad Dahab (Nehlig et al. 1999). Riofinex Geological Mission evaluated the gold placer deposits in the Murayjib region and concluded that they are economically unimportant (Boyle et al. 1984). Placer deposit in the streams at the old Hamdah mine area (resources of 0.911 million tons containing average of 2.89 g/t gold) was considered by Collenette and Grainger (1994) as possible resources for small mining operations. In 1976, the US Geological Survey Saudi Arabia Mission studied the placer gold-bearing stream sediments and estimated reserves of 0.710 million m^3 containing 0.102 g/m^3 gold at Mahd Ad Dahab (Sahl et al. 1999). Al-Safarjalani (2004) was able to report some significant gold anomalies especially in the upper cycle of the Late Miocene–Pliocene Hofuf Formation in eastern Saudi Arabia (up to 24 g/t at Haradh town).

Methodology

In order to have an idea about some sedimentological characteristics of the collected stream samples, they were subjected to mechanical analysis that can give some important parameters like those of mean grain size, sorting, skewness, kurtosis, etc. Some of the yielded fine-grained fractions were subjected to mineral separation by the convenient methods (separation either by the Frantz isodynamic separator or heavy liquids). This furnishes heavy mineral concentrate or heavy fractions that bear most of the economic gold and other economic minerals such as zircon and monazite.

The heavy fractions were studied microscopically in both thin and polished sections in order to distinguish the opaque and non-opaque minerals. This study was to specify the common Fe–Ti oxide minerals and their alteration products, in addition to free gold and other heavy minerals such as zircon, monazite and thorite. These minerals were studied by the scanning electron microscope (SEM) attached with energy-dispersive X-ray unit (EDX) that made the spot micro-chemical analysis of these heavy minerals possible.

Gold content in the sieved samples was determined to show the magnitude of gold enrichment in the heavy fractions. Amounts of heavy fractions themselves were calculated as figure index that can configure the ratio between heavy minerals to the light ones in a sample and hence gives good expression about gold content in the analysed stream fractions.

Field observations

Vast areas of Al Wajh and Al Muwaylih quadrangles in NW Saudi Arabia are covered by Neoproterozoic basement crystalline rocks. General geology of the NW part of Saudi Arabia is given in Fig. 2 (Vazquez-Lopez and Motti 1981). Detailed geological maps of Al Wajh and Al Muwaylih quadrangles were constructed by Davies (1985) and Davies and Grainger (1985), respectively. The generalized geological map of Al Wajh quadrangle that includes the three studied wadis at the present stage of work is given in Fig. 3 (Davies 1985). It shows high and rugged topography, and the width of the coastal plain becomes narrower on the road from Al Wajh towards Duba. The Phanerozoic sedimentary rocks are situated at both Azlam basin and the coastal plain, and they range in age from the Cretaceous to the recent. Much older sedimentary successions are found at Al Wajh quadrangle in its northeastern extremity, being represented by Paleozoic sandstones. Brief description for both the sedimentary rocks and the Precambrian basement rocks of the quadrangle is given with special emphasis on the wadi terraces and alluvium that contain the placer minerals. Field works have been carried out included several stations in the three wadis (Wadi Al Miyah, Wadi Haramil and Wadi Thalbah; Figs. 4a–c; Table 1).

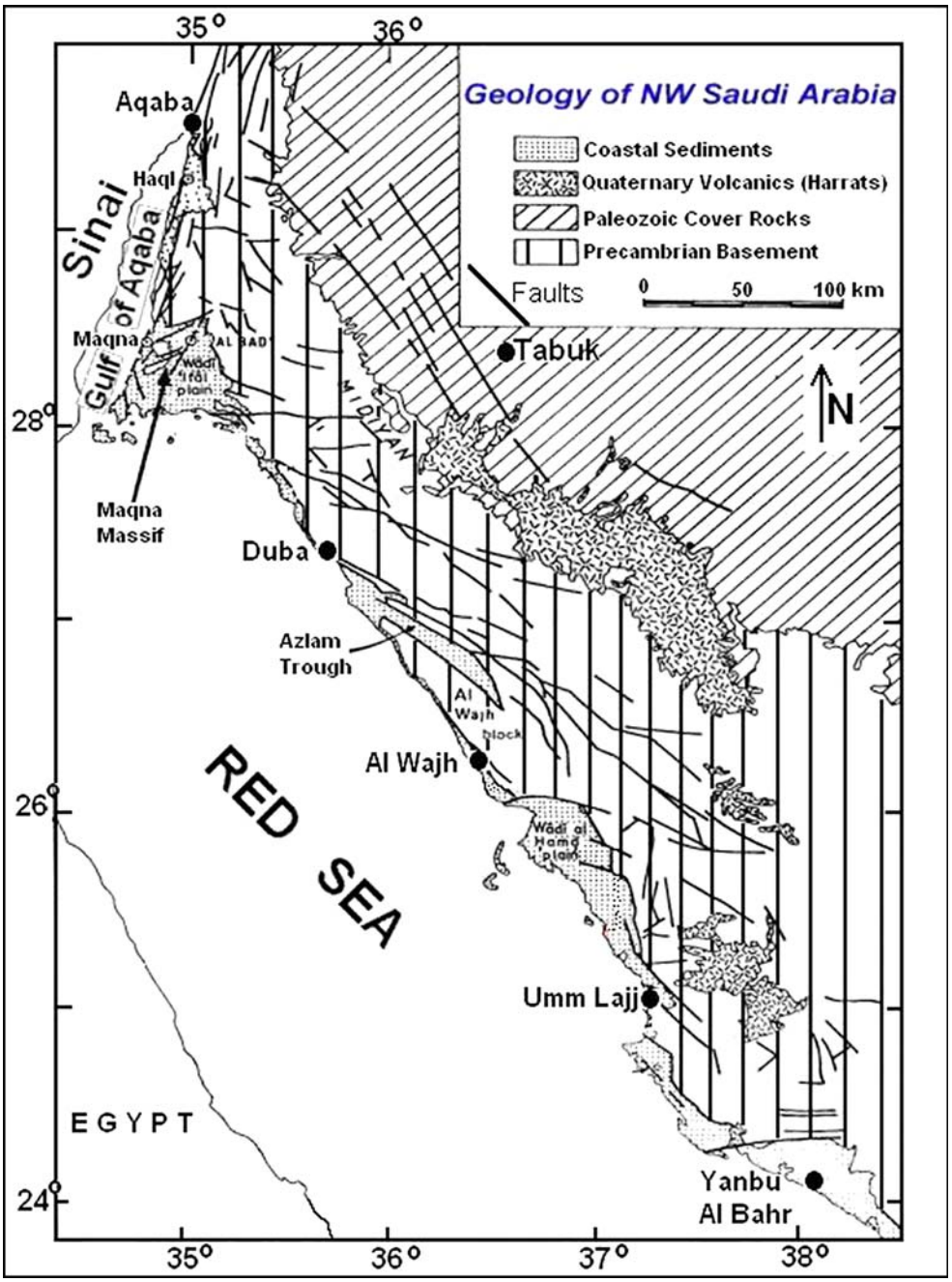

Fig. 2 Geology of NW Saudi Arabia (from Vazquez-Lopez and Motti 1981)

At Wadi Al Miyah, the Precambrian metavolcanics at its eastern extremity, are mostly represented by massive basalt to basaltic andesite covered by Holocene terraces especially in the small tributaries. It is evident that the massive metabasalt is sheared within a 400-m-wide gold-bearing (auriferous) shear zone. At the western extremity of Wadi al Miyah, there are several exposures of pink-coloured granites that range in composition from syeno- to monzogranite. A cut of Quaternary sediments at Wadi Al Miyah was exposed because of a new bridge construction (Fig. 5a). It was possible to report a 5.40-m-deep profile showing different stages and components of the wadi fill (Fig. 5b,c). Figure 5b provides a close view for the profile showing a 90-cm-thick red zone made up of hematitic clay and angular basement pebbles with the presence of thin grey claystone veneers. Raised beach terraces made up of Quaternary coralline limestone are reported at the downstream of Wadi Al Miyah.

Concerning the Wadi Haramil Quaternary beach sediments, there is truncated reefal limestone. Sub-rounded microdiorite pebbles in the limestone are recorded in addition to fossilized echinoid spins in the limestone. The Precambrian molasses-type sediments at the central and eastern parts of the Wadi Haramil that are cut by several quartz veins were identified in the field.

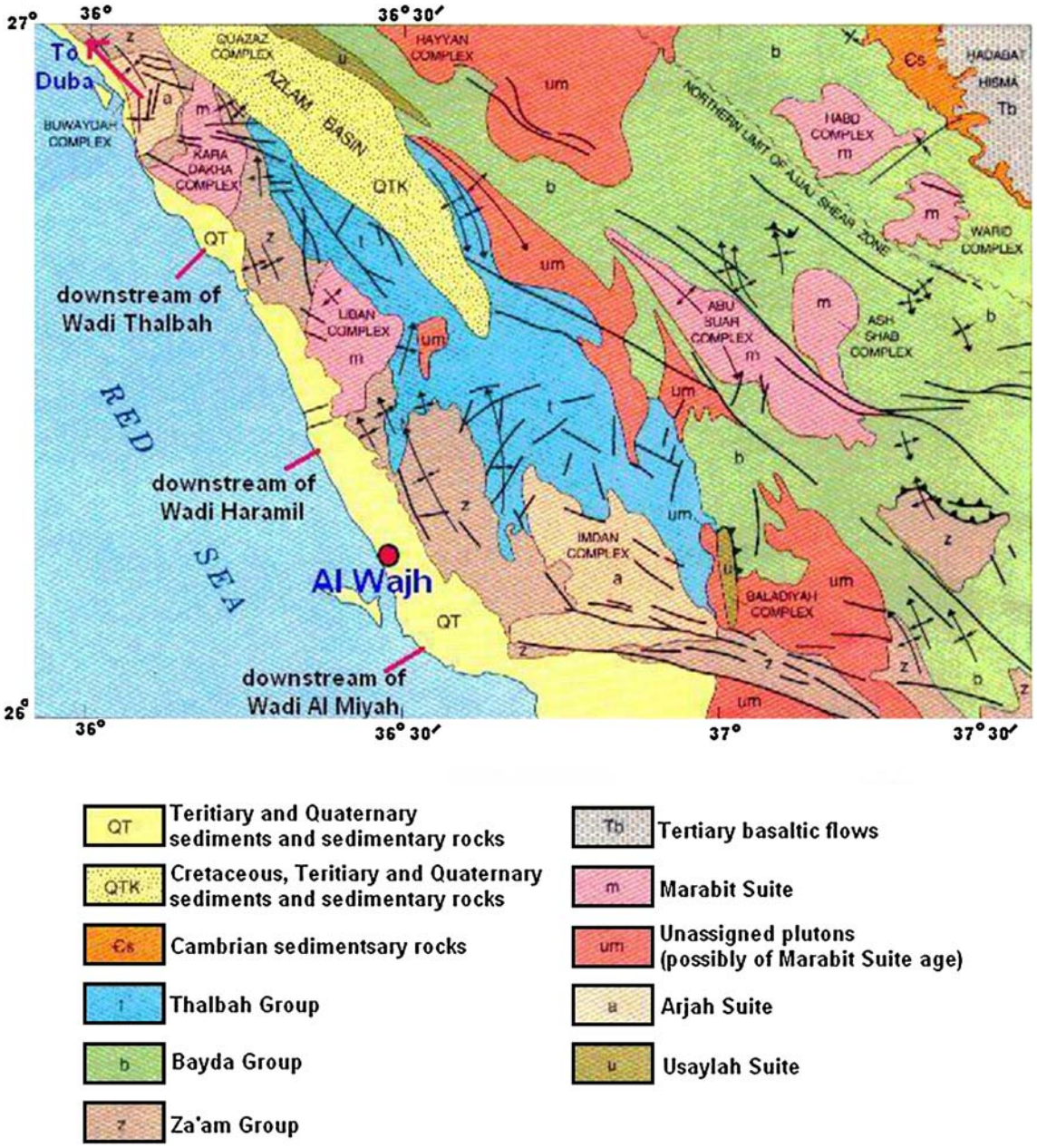

Fig. 3 Generalized geological map of Al Wajh quadrangle (from Davies 1985)

At Wadi Thalbah, the Miocene and Quaternary sediments of Wadi Thalbah at the junction with Azlam basin were detected. There are Quaternary coralline limestone and recent brine and crystalline salts at the wadi course. There are also claystone and anhydrite beds belonging to the Raghama Formation of Miocene age. The Holocene–recent terraces of Wadi Thalbah are common at its middle part, and Fig. 6a is a general view for the terraces on the western side of the main wadi course. In many instances, the eroded terraces are partly covered by windblown sand (Fig. 6b). They are characterized by traces of lamination and the presence of pebbles (Fig. 6c) and the cross-lamination (Fig. 6d). The western parts of the coastal sediments at Wadi Thalbah are represented by clastics of Miocene Raghama Formation non-conformably overlying the Precambrian Za'am group (Fig. 7a). The wadi filling shows lamination and different kinds of pebbles (Fig. 7b). The rippled black sand is directly recorded on the beach (Fig. 7c) where the black sheets of Fe–Ti oxides cap light-coloured beach sediments rich in heavy minerals (mainly zircon and monazite, Fig. 7d).

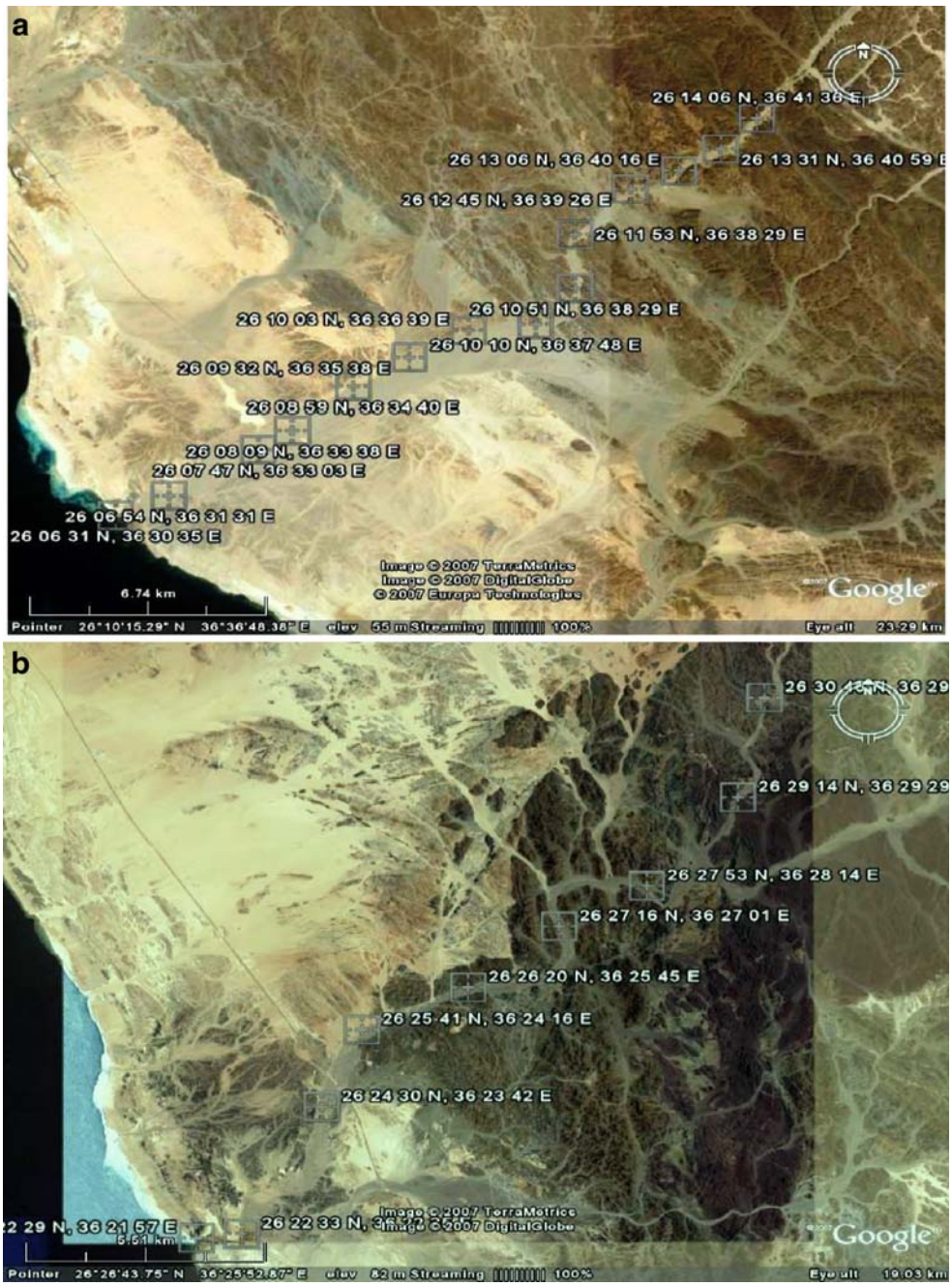

Fig. 4 **a** Sample locations at Wadi Al Miyah. **b** Sample locations at Wadi Haramil. **c** Sample locations at Wadi Thalbah

Fig. 4 (continued)

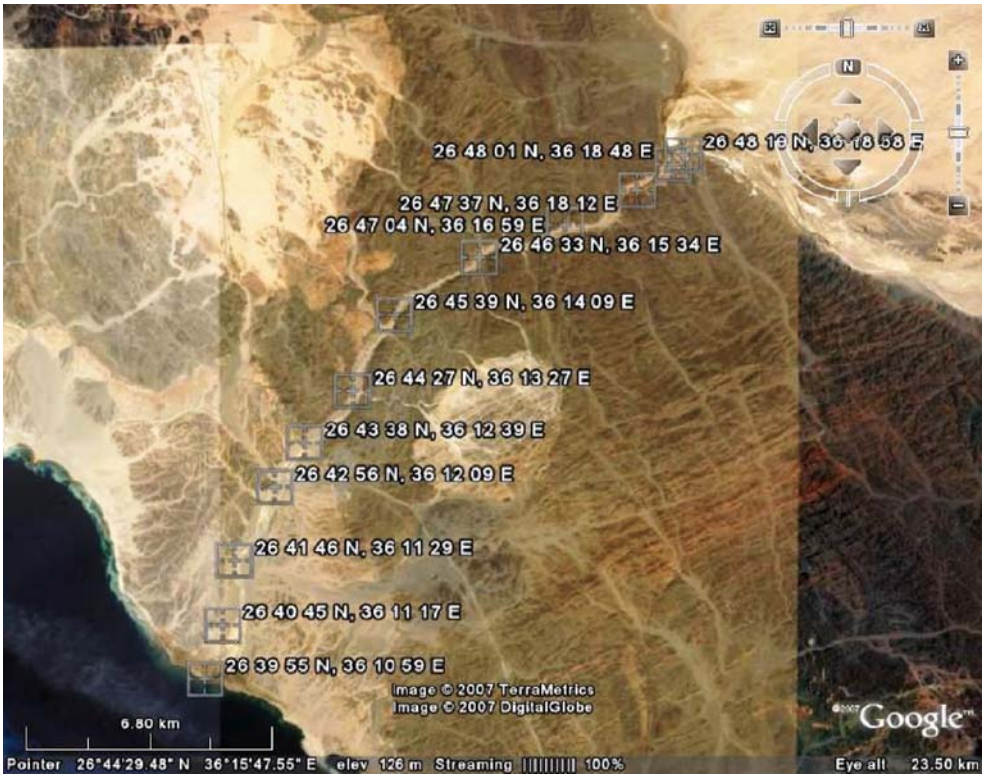

Mechanical analysis

The stream sediments and the mineralogical investigation of the non-opaque fraction have been studied. It shows the concentration of heavy minerals in the studied sediments using heavy liquids and magnetic separation. Also, an account on the chemistry of heavy minerals in the heavy fraction is given based on spot SEM–EDX microanalyses. Grain size analysis was performed for 42 samples collected from the three surveyed wadis (Figs. 4, 6 and 8), three samples from each. About 2–4 kg of each sample is quartered and subjected to screening on a phi set of standard sieves attached to a rotating shaker for about 20 min. The statistical grain size parameters are determined according to the formulae given by Folk and Ward (1957). They are the mean size (M_Z), inclusive graphic standard deviation (σ_i), inclusive graphic skewness (SK_i) and inclusive graphic kurtosis K_G.

Mean size (M_Z) is distinctly variable, being represented by fine pebbles, granules and different categories of sands (very coarse to medium). It is clear that coarse sand is the most frequent fraction (~45%), whereas the least frequent fraction is represented by equal values of fine pebbles and granules (~2%). Medium sand is only reported for five samples (HR2, HR4, HR5, HR6 and HR7) from Wadi Haramil and a single sample from Wadi Al Miyah (MH 25A). The inclusive graphic standard deviation values of the studied stream sediments range from well sorted to very poorly sorted. Statistically, 83.3% of the total studied samples are very well sorted, while 16.67% of samples are well sorted.

It is shown that about 92% of the studied samples are very coarse skewed. Other few samples show nearly symmetrical skewed (HR1, TH1 and TH 10). One sample (HR1) shows finely skewed. Hence, it is evident that the majority of the investigated samples is nearly very coarse skewed, which explains that the addition of finer grains or silting was much minimized. Concerning kurtosis, 75% of the studied samples are represented by the leptokurtic to very leptokurtic classes. Extremely leptokurtic class is encountered for MH17 and MH25C. Mesokurtic class characterizes few samples from Wadi Al Miyah (MH25D) and wadi Thalbah (TH1 and TH5). Platykurtic and very platykurtic classes are known for some samples from Wadi Al Miyah only (MH 25A, MH25B, MH26 and MH 29).

Opaque mineralogy

Thirty polished sections out of 60 samples were studied for their opaque minerals content. Fractions of heavy minerals in the grain size ranges of 40–63, 63–125 and 125–250 μm were separated and then studied using a reflected-light microscope. Fractions of heavy minerals in the different size ranges (40–63, 63–125 and 125–250 μm) show remarkable concentrations of opaque minerals (Table 2). The separated fractions were mounted in resin, ground and polished. Opaque minerals of the studied stream sediments

Table 1 Location of studied stream samples (wadi alluvium, wadi terraces, sand dunes and beach sediments including black sands)

Sample number	Name	Location
Wadi Al Miyah		
MH1	Wadi alluvium	26°14′06″ N 36°41′36″ E
MH2	Terraces	26°14′06″ N 36°41′36″ E
MH6	Wadi alluvium	26°13′31″ N 36°40′59″ E
MH8	Wadi alluvium	26°13′06″ N 36°40′16″ E
MH10	Wadi alluvium	26°12′45″ N 36°39′26″ E
MH14	Wadi alluvium	26°11′53″ N 36°38′29″ E
MH17	Wadi alluvium	26°10′51″ N 36°38′29″ E
MH20	Wadi alluvium	26°10′10″ N 36°37′48″ E
MH22	Wadi alluvium	26°10′03″ N 36°36′39″ E
MH23	Wadi alluvium	26°09′32″ N 36°35′38″ E
MH24	Wadi alluvium	26°08′59″ N 36°34′40″ E
MH25	Wadi alluvium	26°08′09″ N 36°33′38″ E
MH26	Wadi alluvium	26°07′47″ N 36°33′03″ E
MH27	Wadi alluvium	26°06′54″ N 36°31′31″ E
MH28	Beach sediments	26°06′31″ N 36°30′35″ E
MH29	Beach sediments	26°06′31″ N 36°30′35″ E
Wadi Haramil		
HR1	Wadi alluvium	26°30′45″ N 36°29′51″ E
HR2	Wadi alluvium	26°29′14″ N 36°29′29″ E
HR3	Wadi alluvium	26°27′53″ N 36°28′14″ E
HR4	Wadi alluvium	26°27′16″ N 36°27′01″ E
HR5	Wadi alluvium	26°26′20″ N 36°25′45″ E
HR6	Wadi alluvium	26°25′41″ N 36°24′16″ E
HR7	Wadi alluvium	26°24′30″ N 36°23′42″ E
HR8	Wadi alluvium	26°22′33″ N 36°22′35″ E
HR9	Beach sediments	26°22′29″ N 36°21′57″ E
Wadi Thalbah		
TH1	Sand dune	26°48′01″ N 36°18′48″ E
TH2	Wadi alluvium	26°48′01″ N 36°18′48″ E
TH3	Terraces	26°47′37″ N 36°18′12″ E
TH4	Terraces	26°47′33″ N 36°16′59″ E
TH5	Wadi alluvium	26°47′33″ N 36°16′59″ E
TH6	Wadi alluvium	26°46′33″ N 36°16′34″ E
TH7	Wadi alluvium	26°45′39″ N 36°18′48″ E
TH8	Wadi alluvium	26°44′27″ N 36°13′27″ E
TH9	Wadi alluvium	26°43′38″ N 36°12′39″ E
TH10	Wadi alluvium	26°42′56″ N 36°12′09″ E
TH11	Wadi alluvium	26°41′46″ N 36°11′29″ E
TH12	Wadi alluvium	26°40′45″ N 36°11′17″ E
TH13	Beach black sand	26°39′55″ N 36°10′59″ E
TH14	Beach black sand	26°39′55″ N 36°10′59″ E

are represented by iron–titanium oxides and sulphides, in addition to some precious metals. Iron–titanium oxide minerals (magnetite, ilmenite and their alterations such as rutile and titanite) exhibit a variety of textures such as exsolution, alteration and replacement textures.

The microscopic description of these opaques will be demonstrated with special emphasis on the mineral microfabrics and textures in order to shed some light on the possible economic potentiality of opaque minerals in the stream sediments in the wadis between Duba and Al Wajh, particularly those in extremity to Al Wajh.

Pale grey magnetite is mostly of titanomagnetite type as revealed by its pinkish tint that increases with increasing titanium content (Buddington 1956; Buddington and Lindsley 1964). It is the main constituent of the opaque minerals in the studied sediments and is represented by homogeneous phase, i.e. free of any exsolutions, though it is represented by very fine skeletal crystals that exhibit a variety of forms, e.g. star-shaped, cruciform, fish bone as well as dissemination in some volcanic rock fragments. Magnetite in the studied stream samples from Wadi Al Miyah, Wadi Haramil and Wadi Thalbah can be classified as follows: homogeneous titanomagnetite, ilmenite–magnetite intergrowths (coarse trellis, sandwich, composite, granules and fine network types) and altered magnetite (martitzation,

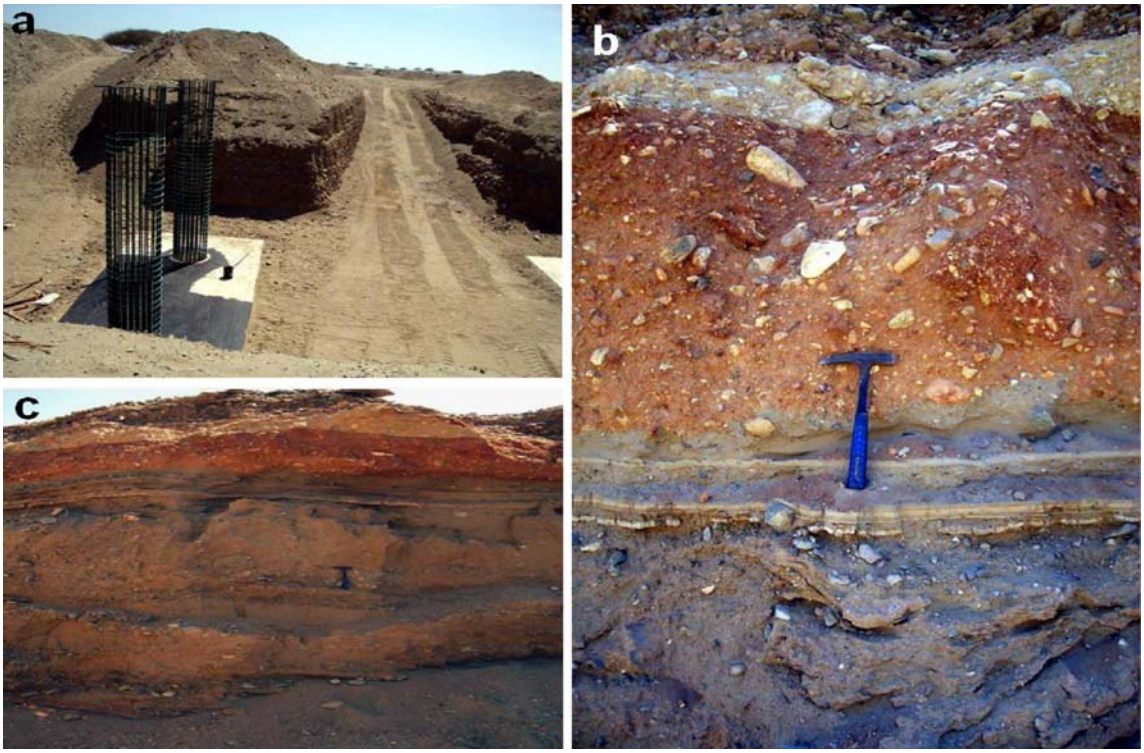

Fig. 5 Quaternary wadi fill of Wadi Al Miyah. **a** Cut of Wadi Al Miyah Quaternary sediments as a result of digging for constructing new bridge at the highway. **b** Close-up view for a 5.40-m-deep profile showing different stages and components of the wadi fill. **c** The profile in the previous photo showing a 90-cm-thick red zone made up of hematitic clay and angular basement pebbles. Note also the presence of thin grey claystone veneers

rutile–hematite intergrowth, replacement by titanite and goethite–limonite intergrowth).

Magnetite exhibits euhedral to anhedral forms indicating that the magnetite is less affected by weathering and transportation. Reynolds (1982), Akimoto et al. (1984), Van der Voo et al. (1993), Xu et al. (1997) and Zhou et al. (1997) have studied the degradation of magnetic oxide minerals in weathered rocks (e.g. the studied magnetite contains inclusions of sulphides and gold).

Detrital opaque oxides show a wide array of textures that result from oxidation, exsolution or primary crystallization (Haggerty 1991). Basu and Molinaroli (1989, 1991) and Darby and Tsang (1987) found that the consideration of exsolution intergrowth textures significantly improved the usefulness of the detrital opaque oxides as provenance discriminators.

Literature review of petrologic observations revealed that alteration of magnetite is more pervasive than that of ilmenite and that both alter to clusters of rutile, hematite and 'limonite' (Temple 1966; Force 1976; Morad 1986). Akimoto et al. (1984) suggested that the alteration process is linked to both the mobility of cations and the oxidation condition. Morad and Aldahan (1986) showed that the alteration of detrital opaques is achieved mainly via dissolution of primary minerals and replacement of these minerals by titanium oxide minerals and hematite. Akimoto et al. (1984) and Van der Voo et al. (1993) demonstrated marked variations in the magnetic properties of rock samples with titanomagnetite, which showed an advanced stage of alteration or total replacement by titanite.

Alteration and replacement textures of magnetite include pre- and post-depositional varieties, in which the latter variety is much more common. The pre-depositional textures of magnetite are normal and heating martitization, titanite, rutile–hematite and pseudobrookite–hematite intergrowth. The post-depositional alterations and replacement are dominated by the formation of goethite and 'limonite.'

Ore-microscopic examination showed that the examined ilmenite grains can be grouped into three main categories namely, homogeneous ilmenite, exsolved ilmenite and altered ilmenite. Ilmenite is abundant in the studied samples but clearly less frequent than magnetite.

In the hematite–ilmenite intergrowths, lamellae of hematite are arranged parallel to the (0001) planes of ilmenite. This type of exsolution is observed in the studied samples. These intergrowths are sometimes termed hemo-ilmenite (Buddington and Balsley 1961). In some cases, the exsolved hematite lamellae are represented by two generations I and II as given by Ramdohr (1960). These lamellae are distributed at the outermost part of the coarse lamellae.

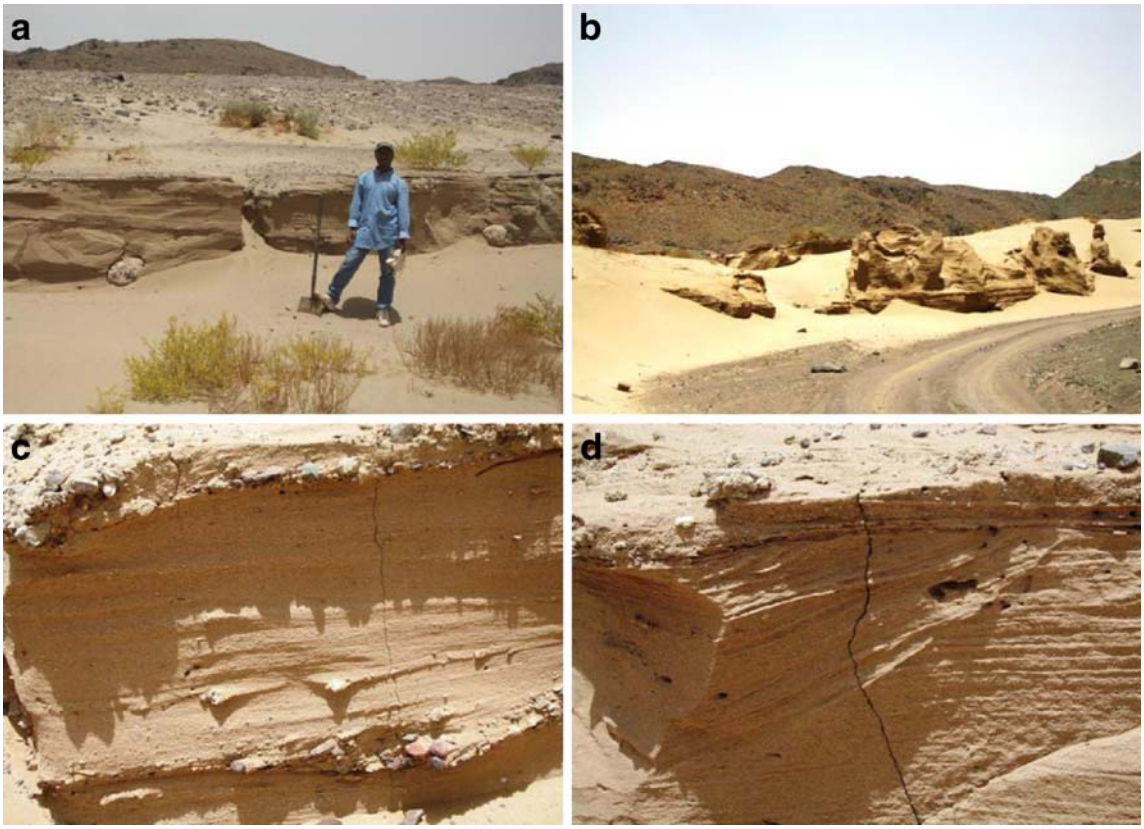

Fig. 6 Holocene–recent terraces of Wadi Thalbah (middle part). **a** General view for the terraces on the western side of the main wadi course. **b** Eroded terraces partly covered by wind-blown sand. **c** Traces of lamination and presence of pebbles in the terraces. **d** Cross-lamination in the relatively coarse-sized terraces

Temple (1966) indicated that alteration of ilmenite in sediments, particularly the sand deposits, is attributed to post-depositional and events of natural processes of weathering rutile–hematite intergrowth represents a type of pre-depositional alterations, and this type of alteration affects both homogeneous and exsolved ilmenite. Rutile–hematite intergrowths result from the oxidation of ilmenite, mostly metamorphism (Ramdohr 1955).

Replacement by titanite is also pre-depositional, and this type of alteration is the most abundance in the studied samples. It is classified, according to the degree of replacement, into slightly altered grains where titanite replaces either part or the border of the grain. Another type of alteration is extensive where titanite replaces most of the grain with the presence of ilmenite relics. These relics are either regular or irregular patches. The replacement of ilmenite by titanite is common in igneous rocks as the result of auto-metasomatism or hydrothermal solutions (Jensen 1966). Post-depositional alterations are mostly represented by 'leucoxene' as ilmenite, which is partly or completely replaced by a mixture of goethite and 'limonite' which forms irregular aggregates as concentric bands.

Figure 8 provide some SEM back-scattered electron image of Fe–Ti oxides and their intergrowths in the heavy fractions. Homogenous ilmenite shows the discontinuous reaction rim to titanite (Fig. 8a). Homogenous ilmenite is altered to titanite enclosed in plagioclase (Fig. 8b). Sometimes, the homogenous ilmenite occurs as a nucleus for carbonate ooids that forms in agitated water near the beach as the case of Wadi Thalbah (Fig. 9). Subhedral homogenous magnetite occurs as disseminations in quartz clasts (Fig. 8c). Figure 8d shows a fine network intergrowth of ilmeno-magnetite in which ilmenite (exsolved) is geometrically arranged in magnetite (host). The coarse-trellis ilmenite–magnetite intergrowth is displayed (Fig. 8e) and also the banded ilmenite–magnetite intergrowth (Fig. 8f). In many cases, the hemo-ilmenite grains contain external silicate and zircon granules (Fig. 8g), and in rare cases, the hemo-ilmenite grains are twinned (Fig. 8h).

Microscopic investigation of the non-opaque minerals

Biotite represents the most abundant mineral among the non-opaques. It is detected in all of the examined samples, but its highest value is reported in the coarse fraction (125–250 μm) and fine fraction (63–125 μm), respectively. Averages of abundance in both fractions are ~9% and ~7%, respectively.

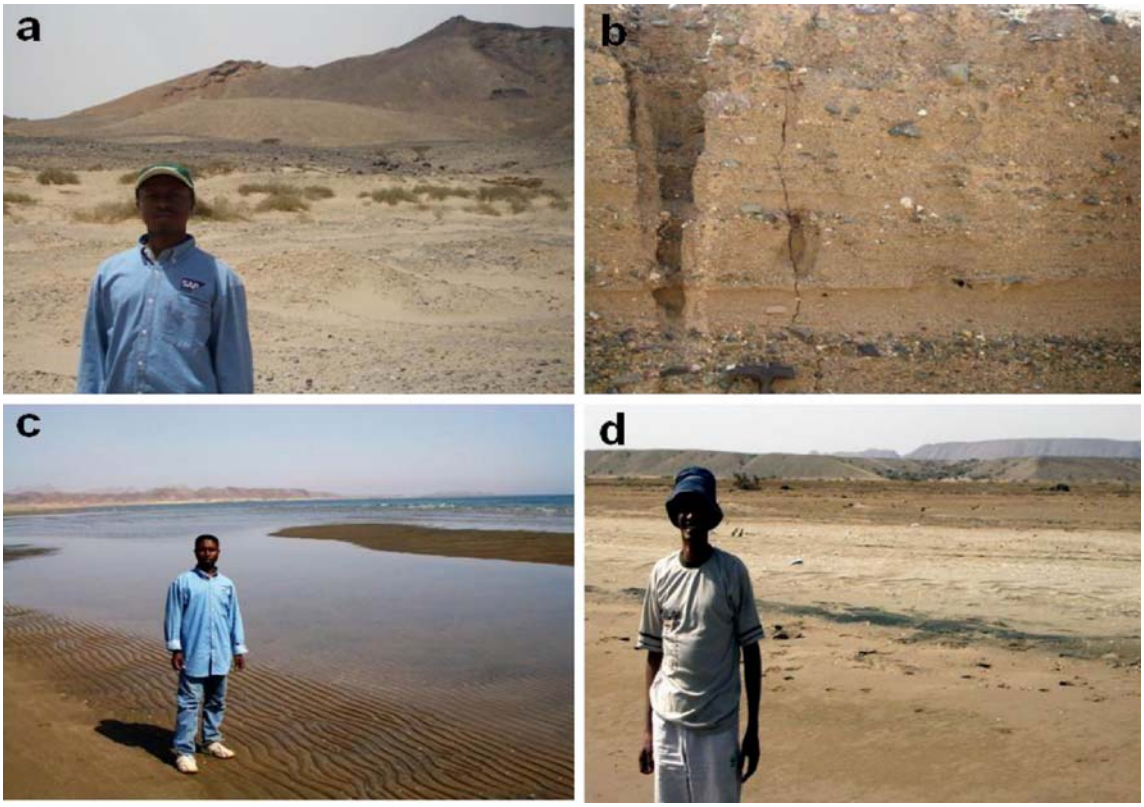

Fig. 7 Coastal sediments of Wadi Thalbah (western part). **a** Clastics of Miocene Raghama Formation (*left*, *light*) non-conformably overlying the Precambrian Za'am group (*right*, *dark*). **b** Wadi filling showing lamination and different kinds of pebbles. **c** Rippled black sand directly on the beach. **d** Dark Fe–Ti oxides capping light-coloured beach sediments rich in heavy minerals (mainly zircon and monazite)

Both hornblende and biotite are brown in colour where the former is the only detected amphibole mineral. The investigated hornblende is most probably derived from the non-ophiolitic or younger gabbros of Al Wajh area (Basyoni and Surour 2006). Brown hornblende or Ti-rich hornblende is either anhedral and equant or subhedral and prismatic. On the other hand, green hornblende is probably derived from the calc-alkaline granitoids or metamorphic rocks. Epidote-group minerals are abundant in the studied sediments and are represented by zoisite and pistachite. It is difficult to distinguish the source of epidote because it could be derived from both felsic and mafic rocks in the hinterlands. Rutile (mostly as mixture with leucoxene) is encountered in most samples, whereas pyroxenes are represented by traces of hypersthene and abundant augite.

Apatite is common in the studied stream sediments. It occurs either as independent crystals or incorporated as inclusions in other minerals. Under the microscope, the apatite crystals are often clear, but some turbid crystals are seldom. It is commonly euhedral, and the outlines are either prismatic or basal six-sided. Fine inclusions of apatite are often enclosed by zircon. Rhombic titanite is common resulting from the replacement of Ti-rich opaques. This is documented by the presence of relict irregular titaniferous opaques in titanite.

Zircon is common in the studied sediments occurring either as short or long prismatic ultrastable crystals with or without bipyrmidal terminations (Fig. 10a). Also, it occurs as fine slender-shaped inclusion in ilmenite (Fig. 10b). Basal tetragonal grains are much less frequent. Colourless to turbid short zircon occurs as zoned euhedral crystals (Fig. 10c). Some short zircon crystals are a bit dark and exhibit dentate outlines which is uncommon for an ultrastable mineral like zircon. The microscopic investigation indicates that some of the studied sediments contain short twinned zircon crystals. In some few cases, the length of zircon is intermediate, being slightly zoned and exhibits different yellow shades.

Monazite is an essential mineral among the non-opaques. The encountered monazite is colourless and pitted. It occurs as subhedral to anhedral prismatic crystals (Fig. 11a) with high relief and very weak birefringence. It is seldom cracked (Fig. 11b) and sometimes are recorded along cracks in silicate minerals (Fig. 11c). With respect to the possible source rocks, monazite is derived from granites and pegmatites that are common in Duba–Al Wajh district (Davies 1985).

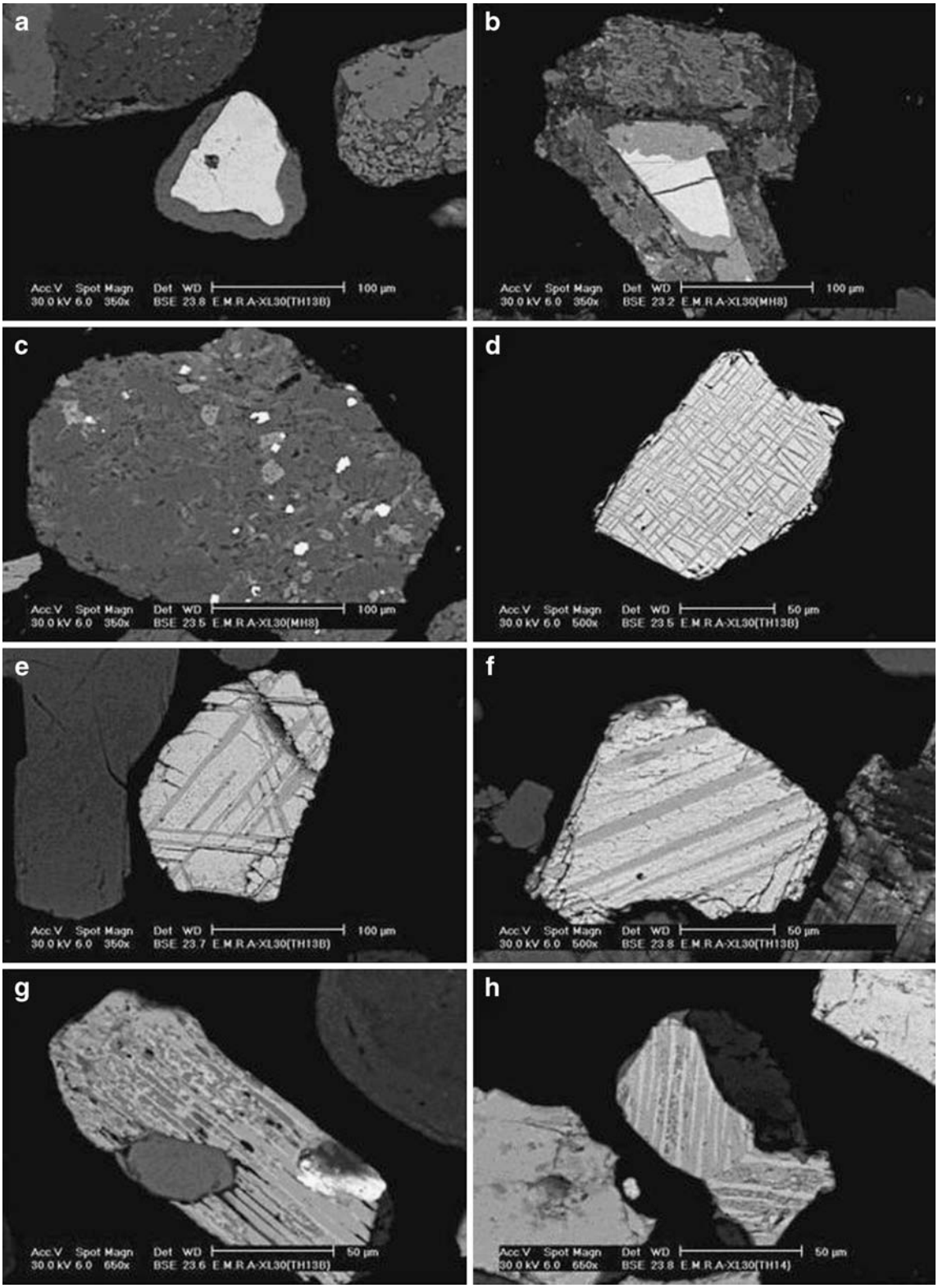

Fig. 8 SEM back-scattered electron image of Fe–Ti oxides and their intergrowths in the heavy fractions. **a** Homogenous ilmenite showing discontinuous reaction rim to titanite, Wadi Al Miyah. **b** Homogenous ilmenite altered to titanite enclosed in plagioclase, Wadi Al Miyah. **c** Subhedral homogenous magnetite disseminations in quartz clast, Wadi al Miyah. **d** Fine network intergrowth ilmenite (*dark lamellae*)–magnetite (*light host*), Wadi Al Miyah. **e** Coarse-trellis ilmenite–magnetite intergrowth, Wadi Al Miyah. **f** Banded ilmenite–magnetite intergrowth, Wadi Al Miyah. **g** Altered hemo-ilmenite grain with external silicate and zircon granules, Wadi Al Miyah. **h** Twinned hemo-ilmenite grain, Wadi Thalbah

Table 2 Ratio of heavy to light minerals calculated as index figure percentage

Name of stream	Sample number	Gross weight (g)	Weight of heavy minerals (g)	Weight of light minerals (g)	Index figure (%)
Wadi Al Miyah	MH1	694.6	34.15	660.45	4.92
	MH6	685.3	12.54	672.76	1.83
	MH8	636.4	49.06	587.34	7.71
	MH14	200	3.9	196.1	1.95
	MH17	452.9	17.35	435.55	3.83
	MH20	100.3	0.3	100	0.30
	MH26	413.8	29.81	383.99	7.20
	MH28	547	3.81	543.19	0.70
Wadi Haramil	HR1	695.6	11.01	684.59	1.58
	HR3	420.4	36	384.4	8.56
	HR5	292.1	13.87	278.23	4.75
	HR9	1280.2	19.22	1260.98	1.50
Wadi Thalbah	TH1	786.6	21.72	764.88	2.76
	TH7	886.2	111.06	775.14	12.53
	TH13A	1213.5	166.62	1046.88	13.73
	TH13B	1223.4	175.17	1048.23	14.32
	TH14	738.4	108.67	629.73	14.72

Radioactive minerals are only represented by thorite, in addition to an uraniferous zircon variety as proved by the mineral chemistry. Thorite itself sometimes contains considerable amounts of uranium and becomes uranothorite. U-poor or U-free thorite occurs as liberated grains that are often cracked (Fig. 12a) with preferential occurrence in the black sands at the downstream of Wadi Thalbah. Uranothorite is much finer in size if compared by the U-poor thorite where the former is hosted by the latter (Fig. 12b,c).

Several particles of native gold were detected during the microscopic investigation. Then, the gold content was estimated by the fire assay technique, just for preliminary estimation. There are two modes for the occurrence of gold in the studied stream sediments. The first was in the form of free gold, which is much common. The second is represented by gold inclusions in other minerals such as in quartz, other silicate minerals and magnetite. Invisible gold often associates sulphide nuclei in magnetite rather than in ilmenite. Ore microscopic investigation suggests that gold is concentrated in the silt fraction (40–63 μm). But, particles of extremely fine "dusty" gold (≤40 μm in size) were also identified in most stations as independent grains.

Mineral chemistry

In order to have some information about the mineral chemistry of some heavy minerals in Duba–Al Wajh stream sediments, some spot EDX microanalysis were carried out. Table 3 gives seven spot analyses of Fe–Ti oxides and their alteration products. The first five analyses are for homogenous ilmenite except for the fifth one, which is an exsolved phase with magnetite, i.e. ilmenite–magnetite intergrowth. No distinct chemical differences can be noticed if homogenous ilmenite is compared to the exsolved one where the contents of Ti, Mn and Fe are almost the same. Only one homogenous ilmenite grain from Wadi Al Miyah (analysis no. 4) contains a doubled value of MnO amounting 6.39 wt%. The chemical composition of magnetite indicates a distinct titanomagnetite variety which is consistent with the ore microscopic investigation. This titanomagnetite contains 3.85 wt% TiO_2. The TiO_2 content in some other grains would be higher, and it increases with the pinkish tint of the mineral in polished sections. This type of titanomagnetite is almost V- and Cr-free, which indicates derivation from a more felsic source than a mafic one. The microanalysis of titanite shows remarkable depletion in MnO content indicating that the Mn^{2+} ions are liberated upon transformation of ilmenite into titanite. In

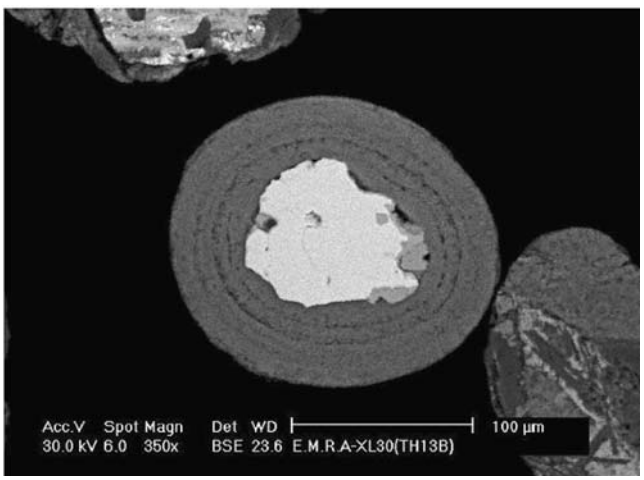

Fig. 9 SEM back-scattered electron image of carbonate ooid composed of homogenous ilmenite (*light*, partly altered to grey titanite) and *dark* outer calcite shells, heavy fractions in the beach sediments of Wadi Thalbah

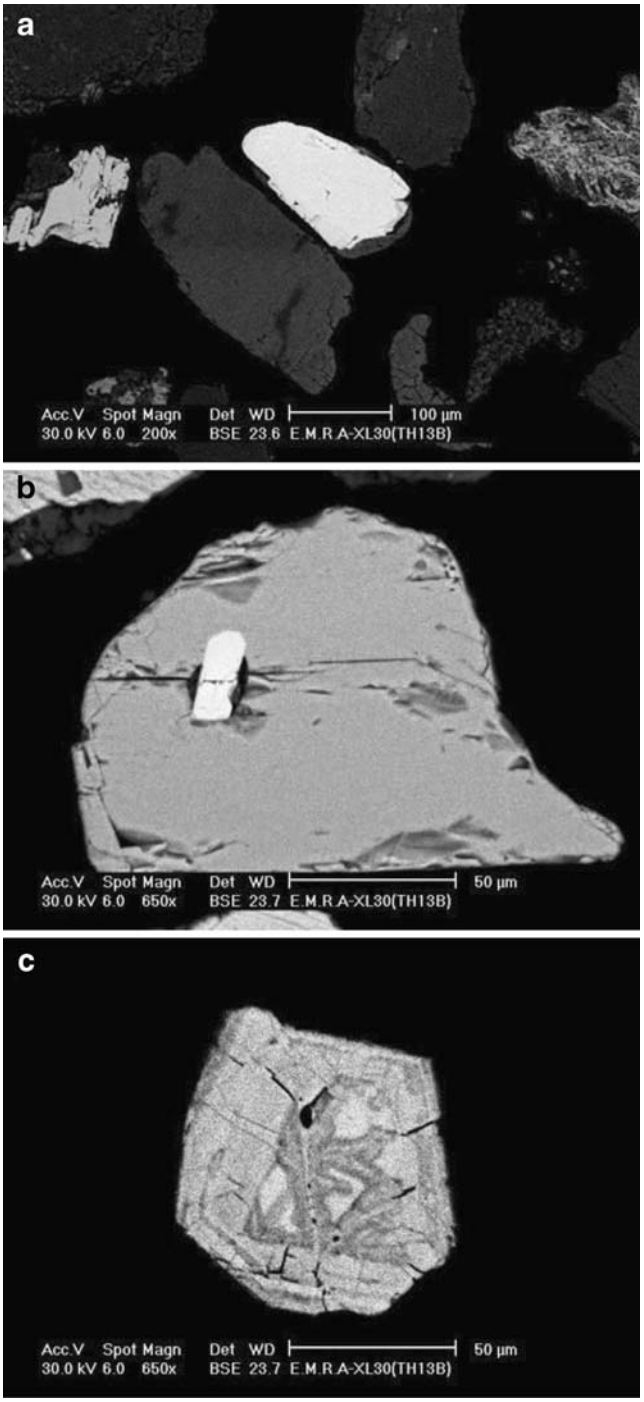

Fig. 10 SEM back-scattered electron images of zircon in the heavy fractions of stream sediments. **a** Non-radioactive Hf-bearing zircon (*light*, *bright*), Wadi Al Miyah. **b** Euhedral zircon enclosed in homogenous ilmenite, Wadi Al Miyah. **c** Zoned zircon showing cracking due to its radioactivity, Wadi Al Miyah

this case, Mn oxide can form Mn staining for other mineral grains, either light or heavy.

The chemical analyses of zircon shows that the mineral is in most U-free and sometimes bear up to 2.74 wt% Hf_2O_3 (Table 4). Ti and Fe impurities (see analysis no. 2 of zircon) result from the composition of Fe–Ti oxide hosting the zircon. Table 5 gives the chemical analyses of two monazite crystals. The first analysis shows some traces of both CaO (1.96 wt%) and Ta_2O_5 (1.16 wt%), where the first can be attributed to the presence of fine apatite inclusions or denotes Ca in the host silicate structure. Both monazite analyses show the typical

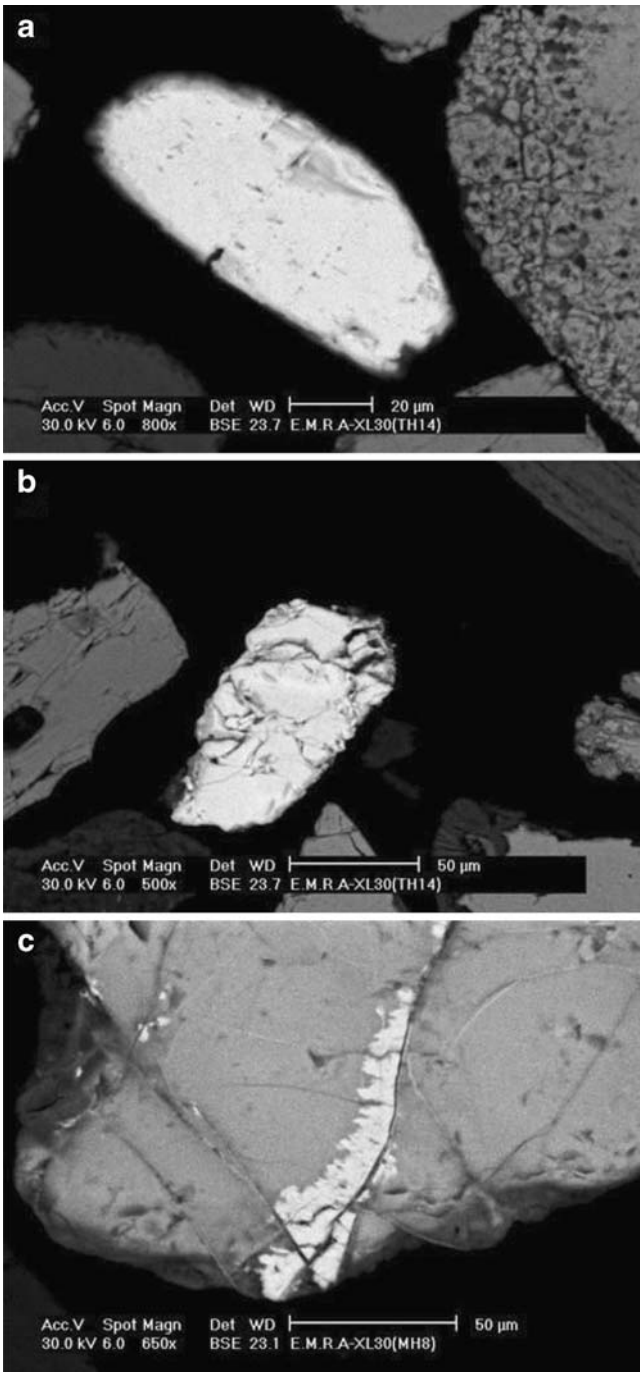

Fig. 11 SEM back-scattered electron images of monazite in the heavy fractions of stream sediments. **a** Corroded monazite prism, Wadi Al Miyah. **b** Cracked monazite, Wadi Thalbah. **c** Monazite (*light*) along cracks in silicates, Wadi Thalbah

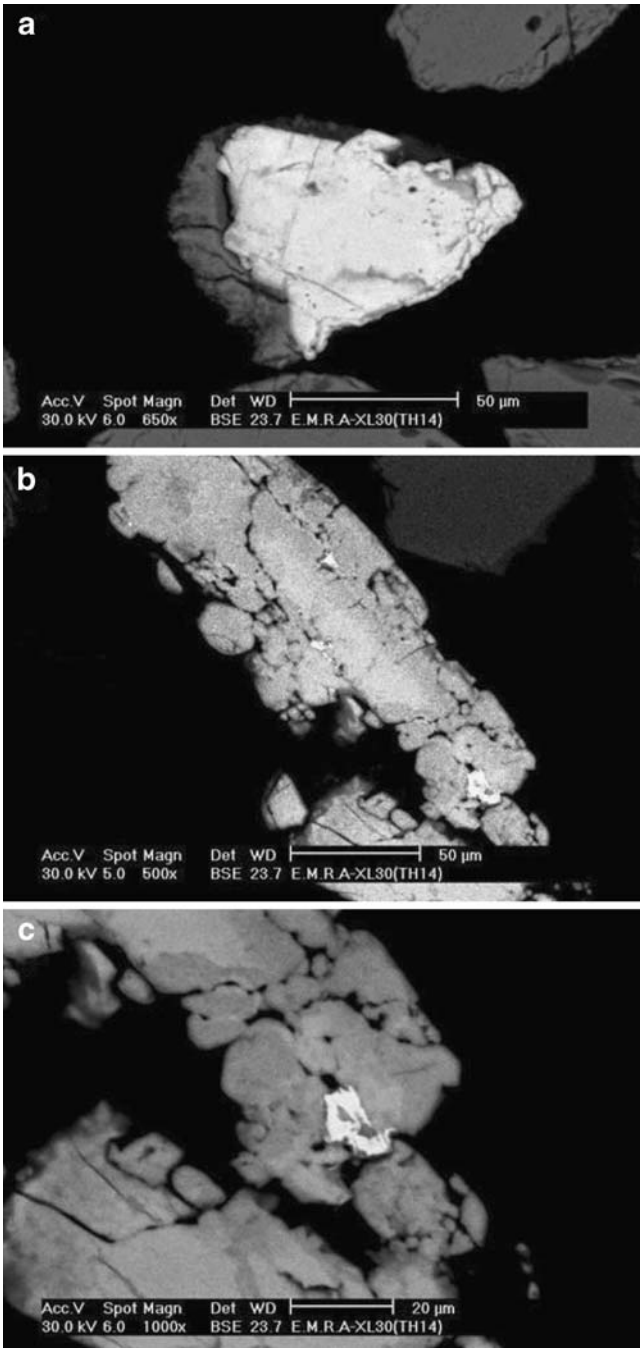

Fig. 12 SEM back-scattered electron images of thorite in the heavy fractions of stream sediments. **a** Slightly cracked free thorite grain, Wadi Thalbah. **b** Uranothorite (*light*) hosted by U-poor thorite (*grey*), Wadi Thalbah. **c** Details of the *lower portion* of the previous photo

common contents of rare earth elements (REE) such as La, Ce, Nd and Sm. Remarkably, high ThO_2 content (6.11–8.13 wt%) results from extremely fine thorite inclusions as indicated by the EDX runs. The chemical analyses of thorite (Table 6) indicate either U-free or uranothorite varieties where the latter contains up to 31.79 wt% UO_2. One of the U-free thorite grains is Y-bearing and contains 7.13 wt% Y_2O_3.

Gold content in Duba–Al Wajh stream sediments

Gold content in the stream sediments of three wadis (located at the southern half of Duba and Al Wajh district) was determined for 20 representative samples from Wadi Al Miyah, Wadi Haramil and Wadi Thalbah. The determination of gold content using the fire assay technique was carried out on sieved samples before mineral separation and in the heavy fractions after separation by the convenient methods.

Data of gold content in the studied stream sediments (Table 7) shows that all sieved unseparated samples are gold-bearing despite of being of low content (0.06–1.40 g/t Au) because gold is diluted by the light minerals. After mineral separation of sample no. TH7B, with 1.40 g/t Au, the grade increases to 28.83 g/t gold because this sample is enriched in sulphides nuclei in magnetite and free gold in heavy rock fragments.

Table 7 shows that the maximum gold content in the samples of Wadi Al Miyah is 13.61 wt% which is reported for the heavy fraction (size A=<40 μm) of sample MH170. So, gold here is more concentrated in the silt-sized fraction like the case of Al Hofuf sediments (Al-Safarjalani 2004) and Wadi Al Hamd stream sediments (Basyoni and Surour 2006; Qadi et al. 2007) of Saudi Arabia.

Maximum gold content in the heavy fractions of Wadi Haramil stream sediments is shown be sample no. HR5 that contains 6.90 g/t Au (Table 7) in a relatively coarse fraction (size C=63–125 μm). The size still fulfills the silt fraction, but the coarsening of gold can be correlated with either the original size of native gold in the Precambrian mineralized zone or/and the distance of transportation.

It appears that the most fertile heavy fractions in gold among the analysed samples are those from Wadi Thalbah that have the highest index figure, which make the placer gold. Except for sample no. TH1 at the upstream with 0.77 g/t Au, the gold content in the rest of the sample is economically high lying in the range 6.27–28.83 g/t Au (Table 7).

Discussion

As far as the author is aware, the present study is the first contribution for studying placer gold in the stream sediments between Duba and Al Wajh. According Davies and Grainger, the Al Wajh Quadrangle itself possesses about 26 gold occurrences (mostly related to NW-trending Najd fault system). Gold mineralization there is mostly represented by Precambrian shield rocks. In the present study, three wadis were surveyed for their auriferous stream sediments. The shield rocks there are represented by wide varieties of rocks, e.g. metavolcanics (massive basalt to basaltic andesite) that are covered by Holocene terraces especially in the small tributaries. The massive metabasalt and its

Table 3 EDX microanalyses of Fe–Ti oxides and titanite

Oxide wt%	Mineral						
	Ilmenite[a]					Magnetite[b]	Titanite (sphene)[c]
	1	2	3	4	5		
TiO_2	49.71	46.31	49.48	49.45	47.69	3.85	37.34
MnO	3.64	3.41	3.89	6.39	3.04	1.01	n.d.
Fe_2O_3	46.65	51.27	46.63	44.17	49.27	95.14	1.30
CaO	–	–	–	–	–	–	30.02
SiO_2	–	–	–	–	–	–	31.34
Total	100	100	100	100	100	100	100

– Not detected

[a] Analysis no. 1 for homogenous ilmenite nucleus in carbonate ooid shown in Fig. 9, Wadi Thalbah; analysis no. 2 for homogenous ilmenite hosting zircon shown in Fig. 8b, Wadi Thalbah, analysis no. 3 for homogenous ilmenite inclusion in biotite, Wadi Al Miyah, analysis no. 4 for homogenous ilmenite, Wadi Al Miyah, analysis no. 5 for exsolved ilmenite in coarse-trellis ilmeno-magnetite intergrowth, Wadi Thalbah

[b] Magnetite hosting ilmenite (analysis no. 5)

[c] Titanite (sphene) replacing homogenous ilmenite (analysis no. 4)

sheared member lie within a 400-m-wide shear zone with common injection of thin quartz stringers at the vicinity of sheared metabasalt. Thinly bedded metabasaltic tuff is also common, in addition to several exposures of the Thalbah Group (Precambrian conglomerate, litharenite and mudstone), pink granites ranging in composition from syeno- to monzogranite and rhyodacite to rhyolite sills and dykes. The coastal sediments are represented by clastics of Miocene Raghama Formation non-conformably overlying the Precambrian Za'am group. The wadi filling shows lamination and different kinds of pebbles. The rippled black sand is directly recorded on the beach where the black sheets of Fe–Ti oxides cap light-coloured beach sediments rich in heavy minerals (mainly zircon and monazite). The beach is mostly occupied by Quaternary reefal limestone with occasional crinoidal stems. At Wadi Thalbah, the Miocene and Quaternary sediments of Wadi Thalbah at the junction with Azlam basin were detected. There are Quaternary coralline limestone and recent brine and crystalline salts at the wadi course. There are also claystone and anhydrite beds belonging to the Raghama Formation of Miocene age characterized by alternation of gypsum (replaced by anhydrite) and fine brown mud.

Checking the Tertiary and Quaternary rocks at Wadi Al Hamd (just at the south junction with Wadi Al Miyah) revealed that there is polymectic conglomerate terminated by bedded quartz–arenite. The Quaternary polymectic conglomerate overlies the Tertiary claystone along the unconformity surface, whereas Holocene terraces are accumulated at the footslope of Quaternary terraces. The Holocene terraces are thinly laminated friable Holocene terraces that display perfect cross-lamination. From the chemical point of view, there is no distinct chemical differences between homogenous and exsolved ilmenite. The microscopic investigations prove the presence of many types of ilmenite–magnetite exsolution textures, e.g. fine network, coarse trellis, banded and sandwich types. Chemical composition of magnetite indicates a distinct titanomagnetite variety (with TiO_2 amounting 3.85 wt%), which is consistent with the ore microscopic investigation. The titanomagnetite is almost V- and Cr-free, which

Table 4 EDX microanalyses of zircon

Oxide wt%	Analysis number	
	1	2
SiO_2	39.46	39.53
ZrO_2	57.80	57.02
Hf_2O_3	2.74	–
TiO_2	–	1.05
Fe_2O_3	–	2.40
Total	100	100

– Not detected

Analysis no. 1 for zircon shown in Fig. 10a, Wadi Thalbah; analysis no. 2 for zircon hosted by ilmenite shown in Fig. 10b, Wadi Thalbah

Table 5 EDX microanalysis of monazite[a]

Oxide wt%	Analysis number	
	1	2
P_2O_5	30.94	28.21
CaO	1.96	–
La_2O_3	15.87	19.38
Ce_2O_3	29.43	31.62
Nd_2O_3	12.89	11.55
Sm_2O_3	1.64	1.11
Ta_2O_5	1.16	–
ThO_2	6.11	8.13
Total	100	100

[a] Both analysed grains are from Wadi Thalbah

Table 6 EDX microanalysis of thorite

Oxide wt%	Analysis number			
	1	2	3	4
ThO_2	75.96	64.85	56.86	49.86
SiO_2	19.06	22.24	11.69	7.01
CaO	2.94	2.29	3.58	3.38
Fe_2O_3	2.04	3.50	3.43	2.58
Y_2O_3	–	7.13	–	–
P_2O_5	–	–	6.28	5.38
UO_2	–	–	18.16	31.79
Total	100	100	100	100

– Not detected

Analysis no. 1 for U- and Y-free thorite, Wadi Thalbah; analysis no. 2 for Y-bearing thorite, Wadi Thalbah; analysis no. 3 for uranothorite as inclusions in U-free thorite, Wadi Thalbah

indicates derivation from a more felsic source than a mafic one. The chemical analyses of zircon shows that the mineral is in most U-free and sometimes bear up to 2.74 wt% Hf_2O_3. Chemical analyses of monazite show typical common contents of REE such as La, Ce, Nd and Sm. Remarkably high ThO_2 (6.11–8.13 wt%) may be regarded to fine thorite inclusions. The chemical analyses of thorite indicate either U-free or uranothorite varieties where UO_2 in the latter amounts up to 31.79 wt%. One of the U-free thorite grains (sample no. TH13B) is Y-bearing and contains 7.13 wt% Y_2O_3.

Based on the microscopic study, gold in the studied stream sediments occurs either as common free gold or as inclusions in other minerals such as in quartz, and silicates and magnetite. On the other hand, invisible gold often associates sulphide nuclei in magnetite rather than in ilmenite. Combined ore microscopic study and fire assay data suggest that gold is concentrated in the silt fraction (40–63 μm). But, particles of extremely fine 'dusty' gold (≤40 μm in size) were also identified in most stations as independent grains. The maximum gold content in the samples of Wadi Al Miyah is 13.61 wt%, which is reported for the heavy fraction (<40 μm). Maximum gold content in the heavy fractions of Wadi Haramil stream sediments amounts 6.90 g/t Au in a relatively coarse fraction (63–125 μm). The size still fulfills the silt fraction, but the coarsening of gold can be correlated with either original size of native gold in the Precambrian mineralized zone or/and distance of transportation.

Conclusions

According to the work materialized in the present paper, the following concluding remarks can be summarized. Mineral chemistry of magnetite indicates a distinct titanomagnetite variety (with 3.85 wt% TiO_2), which is consistent with the ore microscopic investigation. The titanomagnetite (with 3.85 wt% TiO_2) is V- and Cr-free, which indicates derivation from a more felsic source than a mafic one. No traces of U were found in zircon that sometimes bears up to 2.74 wt% Hf_2O_3. Chemical analyses of monazite show typical common contents of REE such as La, Ce, Nd and Sm. Thorite is either U-free or uranothorite varieties where the latter contains up to 31.79 wt% UO_2. One of the U-free thorite grains is Y-bearing and contains 7.13 wt% Y_2O_3.

The conclusions of this paper are as follows:

1. The studied heavy fractions containing articles of extremely fine 'dusty' gold (≤40 μm in size) were identified in most stations as independent grains. The maximum gold content in the samples of Wadi Al Miyah is 13.61 wt%, which is reported for the heavy fraction (<40 μm).
2. Maximum gold content in the heavy fractions of Wadi Haramil stream sediments amounts up to 6.90 g/t Au in a relatively coarse fraction (63–125 μm).
3. Gold content in the heavy fractions of samples from Wadi Thalbah is economically high lying in the range 6.27–28.83 g/t Au, except for a sample collected upstream with 0.77 g/t Au.

Table 7 Gold content (g/t) in raw samples and their heavy fractions

Name of stream	Sample number	Size category[a]	Au content (g/t) of raw sample	Au content (g/t) of heavy fraction
Wadi Al Miyah	MH1	B	0.21	1.20
	MH6	A	0.20	1.40
	MH8	C	0.20	1.00
	MH14	A	0.36	1.13
	MH17	A	0.66	2.90
	MH20	A	0.68	3.29
	MH26	B	0.60	9.07
	MH28	B	0.30	9.40
	MH170	A	0.66	13.61
Wadi Haramil	HR1	B	0.18	1.40
	HR3A	C	0.18	0.88
	HR3B	B	0.16	0.51
	HR5	C	0.22	6.90
	HR9	D	0.06	0.30
Wadi Thalbah	TH1	E	0.16	0.77
	TH7A	B	0.20	6.27
	TH7B	A	1.40	28.83
	TH13A	B	0.70	14.43
	TH13B	C	0.34	10.66
	TH14	B	0.32	10.02

[a] Scale of size categories: A=<40 μm, B=40–63 μm, C=63–125 μm, D=125–250 μm, E=250–500 μm

4. It appears that the most fertile heavy fraction in gold among the analysed samples are those from Wadi Thalbah that have the highest index figure, which makes the placer gold in them more profitable from the economic point of view. The gold content in the rest of sample is economically high lying in the range 6.27–28.83 g/t Au except for a sample with 0.77 g/t.
5. Al Wajh stream sediments (including the beach light and black sands) are also rich in Fe–Ti oxides, rutile and zircon, whereas monazite and thorite are much lesser.
6. Titanomagnetite (with 3.85 wt% TiO_2) is V- and Cr-free, which indicates derivation from a more felsic source than a mafic one.
7. The investigated uranothorite contains up to 31.79 wt% UO_2, whereas U-free thorite contains 7.13 wt% Y_2O_3. Monazite in the studied sediments contains considerable amounts of REE such as La, Ce, Nd and Sm.

References

Akimoto T, Kinoshita H, Furuta T (1984) Electron probe microanalysis study on process of low-temperature oxidation of titanomagnetite. Earth Planet Sci Lett 71:263–278

Al-Safarjalani AM (2004) Placer gold deposits in the Hofuf Formation, the Eastern Province of Saudi Arabia. Research Project no. 4022. King Faisal University, Riyadh, Saudi Arabia

Basu A, Molinaroli E (1989) Provenance characteristics of detrital opaque Fe–Ti oxide minerals. J Sediment Petrol 59:922–934

Basu A, Molinaroli E (1991) Reliability and application of detrital opaque Fe-Ti oxide minerals in provenance determination. In: Morton AC, Todd SP, Haughton PDW (eds) Developments in sedimentary provenance studies. Geological Society Special Publication, vol. 57. British Geological Survey, Keyworth, UK, pp 55–65

Basyoni MH, Surour AA (2006) Sedimentology and economic potentialities of the Red Sea coastal sediments at Umm Lajj area, Saudi Arabia. Final Report of Project no. 201/425 funded by Institute of Research and Consultation (IRC), King Abdulaziz University, Jeddah

Boyle D, Mc K, Atkinson VG, Sayib KA (1984) An evaluation of gold placer deposits in the Murayjib region. Open-File-Report by Riofinex, RF-OF-04-28, Ministry of Petroleum and mineral Resources, Jeddah, KSA

Buddington AF (1956) Thermometric and petrogenetic significance of titaniferous magnetite—discussion. Am J Sci 254:506–515

Buddington AF, Balsley JR (1961) Micro-intergrowths and fabrics of iron–titanium oxide minerals in some Adirondack rocks. Mehaveden 1:1–16

Buddington AF, Lindsley DH (1964) Iron–titanium oxide minerals and synthetic equivalents. J Petrol 2:310–357

Collenette P, Grainger DJ (1994) Mineral resources of Saudi Arabia (not including oil, natural gas and sulfur). DGMR Special Publication SP-2. Ministry of Petroleum and Mineral Resources, Jeddah, Saudi Arabia

Darby DA, Tsang YW (1987) Variation in ilmenite element composition within and among drainage basins: implications for provenance. J Sediment Petrol 57:831–838

Davies FB (1985) Explanatory notes on the geologic map of Al Wajh quadrangle, Sheet 26 B. Ministry of Petroleum and Mineral Resources, Deputy Ministry for Mineral Resources, Jeddah, Saudi Arabia, p 27

Davies FB, Grainger DJ (1985) Explanatory notes on the geologic map of Al Muwaylih quadrangle, Sheet 27A. Ministry of Petroleum and Mineral Resources, Deputy Ministry for Mineral Resources, Jeddah, Saudi Arabia, p 31

Folk RL, Ward WC (1957) Brazos river bar: a study in the significance of grain size parameters. J Sediment Petrol 27:3–26

Force ER (1976) Metamorphic source rocks of titanium placer deposits—a geochemical cycle. USGS Prof. Paper no. 959-B, p.16

Google Images (2008) Updated satellite images of the Planet Earth from the internet site. www.Google.com

Haggerty SE (1991) Oxide textures—a mini atlas. In: Lindesley DH (ed) Oxide minerals: petrologic and magnetic significance. Reviews in mineralogy, vol. 25. Mineralogical Society of America, Chantilly, VA, pp 129–219

Jensen A (1966) Mineralogical variations across two dolerite dykes from Bornholm. Særtrzk af Maddlelelsor fra Dansk Geologisk, Denmark, pp 370–451

Morad SA (1986) SEM study of authigenic rutile, anatase and brookite in Proterozoic sandstones from Sweden. Swed Geol 46:77–89

Morad SA, Aldahan AA (1986) Alteration of detrital Fe–Ti oxides in sedimentary rocks. Geol Soc Amer Bull 97:567–578

Nehlig P, Salpeteur I, Asfirane F, Bouchot V, Eberlé JM, Genna A, Kluyver HM, Lasserre JL, Nicol N, Recoche G, Shanti M, Thiéblemont D, Tourliere B, the Arabian Shield Project Participants (1999) The mineral potential of the Arabian shield: a reassessment. In: Proceedings of the IUGS/UNESCO Meeting on the "Base and Precious Metal Deposits in the Arabian Shield", Jeddah, November, 12–19

Qadi TM, Surour AA, Maddah SS, Basyoni MH (2007) Mineralogy and economic evaluation of gold-bearing stream sediments from Wadi Al Hamd area, northwestern Saudi Arabia. Ann Geol Surv Egypt 29:209–236

Ramdohr P (1955) Die erzmineralien und ihre verwachsungen. Akadenie, Berlin, p 875

Ramdohr P (1960) Die erzmineralen und ihre verwachsungen, 3rd edn. Akadenie, Berlin, p 1089

Reynolds RL (1982) Post-depositional alteration of titanomagnetite in Miocene sandstone, south Texas (U.S.A.). Earth Planet Sci Lett 61:381–391

Sahl MSA, Al-Shanti AM, Tawfiq MA (1999) Evolution of mineral exploration in the Kingdom of Saudi Arabia during a hundred of years. Minstery of Petroleum and Mineral Resources, Kingdom of Saudi Arabia, (in Arabic)

Temple AK (1966) The alteration of ilmenite. Econ Geol 61:695–711

Van Der Voo R, Fang W, Wong Z, Suk D, Peacor DR, Liong Q (1993) Paleomagnetic and electron microscopy of the Eneishan basalts Yunnan, China. Tectonophysis 221:367–379

Vazquez-Lopez R, Motti E (1981) Prospecting in the sedimentary formations of the Red Sea coastal plain between Yanbu al Bahr and Maqna, 1968–1979. Saudi Arabian Deputy Ministry for Mineral Resources Technical Record, BRGM-10-1

Xu W, Van Der Voo R, Peacor M, Beaubouef RT (1997) Alteration and dissolution of fine-grained magnetite and its effects on magnetization of the ocean floor. Earth Planet Sci Lett 151:79–288

Zhou W, Van Der Voo R, Peacor DR (1997) Single-domain and super paramagnetic titanomagnetite with variable Ti content in younger ocean-floor basalts: no evidence for rapid alteration. Earth Planet Sci Lett 150:353–362